Available online at www.sciencedirect.com
SCIENCE DIRECT®
PERGAMON
International Journal of Heat and Mass Transfer 46 (2003) 3865–3880
International Journal of HEAT and MASS TRANSFER
www.elsevier.com/locate/ijhmt

Thermal entry flow for a viscoelastic fluid: the Graetz problem for the PTT model

P.M. Coelho [a], F.T. Pinho [a], P.J. Oliveira [b,*]

[a] Centro de Estudos de Fenómenos de Transporte, DEMEGI, Faculdade de Engenharia, Universidade do Porto, R. Roberto Frias, 4200-465 Porto, Portugal

[b] Departmento de Engenharia Electromecânica, Universidade da Beira Interior, 6201-001 Covilhã, Portugal

Received 22 January 2002; received in revised form 15 March 2003

Abstract

A theoretical study of the entrance thermal flow problem is presented for the case of a fluid obeying the Phan-Thien and Tanner (PTT) constitutive equation. This appears to be the first study of the Graetz problem with a viscoelastic fluid. The solution was obtained with the method of separation of variables and the ensuing Sturm–Liouville system was solved for the eigenvalues by means of a freely available solver, while the ordinary differential equations for the eigenfunctions and their derivatives were calculated numerically with a Runge–Kutta method.

The scope of the present study was quite wide: it encompassed both the plane and axisymmetric geometries for channel and tube flows; two types of thermal boundary conditions with either an imposed wall temperature or an applied heat flux; inclusion of viscous dissipation; and elastic (through the Weissenberg number) and elongational (through the PTT parameter ϵ) effects. The main underlying assumptions were those of constant physical properties, negligible axial heat conduction, and fully developed hydrodynamic conditions. The results are discussed in terms of the main effects brought about by viscoelasticity and viscous dissipation on the Nusselt number variation and the bulk temperature.

1. Introduction

The problem of determining the thermal characteristics of a fluid entering an heated section along a straight duct has been studied by a number of authors (see e.g. Eckert and Drake [1]) for the particular case of laminar Newtonian flow. When the Prandtl number characterising the physical properties of the fluid is much larger than unity, one can assume that the hydrodynamic conditions at inlet are fully developed and it has then been possible to derive analytical expressions for the evolution of the Nusselt number and the temperature distribution in the cross-section as the fluid enters the heated region. This problem has been known as the "Graetz problem" since Graetz [2,3] solved it in 1883 and 1885 for Newtonian fluids; later, in 1910, Nusselt [4] independently analysed the same problem in such great detail that some texts refer to it as the "Graetz–Nusselt problem". More recent works, where additional references on the subject can be found, are those of Brown [5], who provided highly accurate tabulated data for the necessary eigenvalues and eigenfunctions involved, and Ou and Cheng [6] who analysed the situation with viscous dissipation and also under turbulent flow regime.

For non-Newtonian inelastic fluids, a similar problem has been solved for fluids whose viscosity follows a power-law variation with the shear rate of strain $\dot{\gamma}$, that is $\eta = K\dot{\gamma}^{n-1}$, see the book by Bird et al. [7] for solutions neglecting viscous heating and temperature effects on flow properties. Account of temperature effects on flow properties was considered by Christiansen et al. [8]

* Corresponding author. Tel.: +351-275329952; fax: +351-275329972.

E-mail addresses: pmc@fe.up.pt (P.M. Coelho), fpinho@fe.up.pt (F.T. Pinho), pjpo@ubi.pt (P.J. Oliveira).

0017-9310/03/$ - see front matter © 2003 Elsevier Ltd. All rights reserved.
doi:10.1016/S0017-9310(03)00179-0

Nomenclature

a	non-dimensional elastic/elongational parameter (Eq. (5))
Br	Brinkman number (Eqs. (11) or (13))
c_p	specific heat
D_H	hydraulic diameter
D/Dt	substantial derivative
k	thermal conductivity
Nu	Nusselt number (hD_H/k)
Pr	Prandtl number
q	heat flux
r	radial or lateral coordinate
R	tube radius or channel half-height
Re	Reynolds number
t	time
T	temperature
u	velocity, axial velocity component
$\overline{U}$	average velocity
x	axial coordinate
x'	normalized axial coordinate ($x^*/4(2-n)^2$)
y_k	functions in the eigenvalue problem
We	Weissenberg number ($\lambda\overline{U}/R$)

Greek symbols

α	thermal diffusivity ($k/\rho c_p$)
η	fluid viscosity
μ_i	eigenvalue
ρ	fluid density
θ	non-dimensional temperature
ϵ	model parameter
λ	relaxation time
$\boldsymbol{\tau}$	stress tensor
χ	mean velocity ratio ($\overline{U}_N/\overline{U}$)
$\boldsymbol{\Psi}$	eigenfunction
$\boldsymbol{\nabla}$	gradient operator

Subscripts and superscripts

b	bulk temperature
fd	fully developed
n	plane ($n=0$) or axisymmetric ($n=1$) conditions
N	Newtonian case
m	index for boundary conditions: $T_w(m=0)$ or $q_w(m=1)$
w	wall
$*$	non-dimensional quantities
0	inlet temperature
95	thermal entry length (95%)

and Christiansen and Craig [9], for power-law fluids and a constant wall temperature, and the solution was numerically obtained. Later, Forrest and Wilkinson [10] have also considered internal heat generation by viscous dissipation coupled with the temperature effects on viscosity for constant heat flux at wall. Due to the complexity of the problem, and especially to the lack of solutions of the related hydrodynamic problem, there is no account of a "Graetz" solution for a viscoelastic fluid. In this case a hydrodynamic fully developed viscoelastic flow enters a uniformly heated section of a duct (with axisymmetric or planar geometry) and one seeks to determine how its temperature will evolve from there on. This is a two-dimensional problem, in which the liquid temperature depends on the lateral and the longitudinal position at a given cross-section. The solution of the energy equation is complicated by the fact that the velocity and stress profiles in the viscoleastic liquid are more involved than those for the Newtonian or non-Newtonian power-law fluids. On the other side, whereas the condition of high Prandtl number is only verified by some Newtonian and power-law non-Newtonian fluids, viscoelastic fluids obeying the differential constitutive equations are mostly very viscous and have extremely high Prandtl numbers, usually exceeding those of viscous Newtonian fluids. Thus, the thermal entry problem here considered is most frequently encountered in a number of practical industrial applications, such as mold filling, polymer extrusion and other polymer processing manipulations, where the fluids under consideration have elastic characteristics.

The particular viscoelastic model chosen for the present analysis is the simplified Phan-Thien and Tanner (PTT) model [11] which has been utilised by numerous authors in simulation studies of polymer melts. Quinzani et al. [12] and Peters et al. [13] have shown that the PTT model can represent with sufficient accuracy, for engineering purposes, the flow of those polymer melts and concentrated solutions. In addition, the hydrodynamic solution for fully developed pipe and channel flow is known [14] and the thermal problem corresponding to the asymptotic situation of the present analysis is also known [15,16]. The hydrodynamic solution in [14] is required for the analysis, and the results in [15,16] are useful for checking the correctness of the present solution.

The mathematical techniques here utilised closely follow those of Graetz [2], Brown [5] and Ou and Cheng [6] in the corresponding problem with a Newtonian fluid. The governing equations are transformed into an eigenvalue problem and this, in turn, is solved by methods appropriate for Sturm–Liouville systems that

appear in such transformation. Our derivation has been patterned along the lines of Mikhailov and Özisik [17]. Some details of the present analytical derivation for the viscoelastic fluid model are given here, together with a complete assessment of the results, especially regarding the effect of elasticity and the coupled effect of elasticity and viscous heating on the development of the thermal solution.

2. Governing equations

The present analysis deals with the problem of determining the thermal development region of a viscoelastic liquid flowing under hydrodynamic fully developed conditions in a duct, of either circular cross-section (the axisymmetric problem, in a tube) or a long rectangular cross-section (the planar problem, in a channel). In order to account simultaneously for these two geometries we shall use the index n to compact information, with $n = 1$ for tube flow and $n = 0$ for channel flow. Also, two types of thermal boundary conditions are considered, distinguished by index $m : m = 0$ for an imposed uniform wall temperature T_w, and $m = 1$ for an imposed uniform heat flux at the wall, q_w. The duct is aligned with the x-axis whose origin $x = 0$ corresponds to the point where the thermal condition is applied (for $x < 0$: $T = T_0$, the bulk temperature at inlet), and the radial or lateral coordinate is denoted by r, with R being either the tube radius or the channel half-width. The fluid motion is assumed to be laminar and rectilinear with local velocity $u(r)$ and temperature $T(r,x)$, and the cross-section average velocity $\overline{U}$ is related to the prescribed flow rate.

The rheological equation of state which determines the stress field is [11]

$$\left(1+\frac{\lambda\epsilon}{\eta}tr\boldsymbol{\tau}\right)\boldsymbol{\tau}+\lambda\left(\frac{\mathrm{D}\boldsymbol{\tau}}{\mathrm{D}t}-\boldsymbol{\tau}\cdot\nabla\mathbf{u}-\nabla\mathbf{u}^{\mathrm{T}}\cdot\boldsymbol{\tau}\right)=\eta(\nabla\mathbf{u}+\nabla\mathbf{u}^{\mathrm{T}}) \tag{1}$$

where λ is the relaxation time, η the viscosity coefficient and ϵ the elongational parameter of the model. For $\epsilon = 0$ this model becomes identical to the well-known upper convected Maxwell (UCM) model which still represents an elastic liquid but with little interest for the present problem: the solution is the same as for a Newtonian fluid. So, ϵ appears as an important parameter characterising the fluid; it imparts shear thinning into the shear viscosity variation and impedes unbounded elongational viscosities in uniaxial extension. In duct flow, viscoelasticity is usually characterised by a Weissenberg number defined as $We \equiv \lambda\overline{U}/R$. Now, since the viscosity coefficient η is assumed to be constant, the velocity field is independent of the temperature field and the hydrodynamic solution under fully developed conditions was given by Oliveira and Pinho [14] as

$$u=\overline{U}\frac{3+n}{2}\frac{\overline{U}_{\mathrm{N}}}{\overline{U}}(1-r^{*2})\left[1+a(1-r^{*2})\right] \tag{2}$$

for the velocity profile ($r^* = r/R$), and

$$\tau_{xr}=-(3+n)\eta\frac{\overline{U}}{R}\frac{\overline{U}_{\mathrm{N}}}{\overline{U}}r^{*} \tag{3}$$

for the shear stress profile. In these equations $\overline{U}_{\mathrm{N}}$ represents the average velocity for the Newtonian fluid subjected to the same pressure gradient (i.e. $\overline{U}_{\mathrm{N}} = -R^2(\mathrm{d}p/\mathrm{d}x)/2^n(3+n)\eta$) so that the parameter $\chi = \overline{U}_{\mathrm{N}}/\overline{U}$ is a dimensionless pressure gradient which was given as the solution of the following cubic equation:

$$\left\{\frac{3-n}{\frac{5}{2}-n}(3+n)^2\epsilon We^2\right\}\left(\frac{\overline{U}_{\mathrm{N}}}{\overline{U}}\right)^3+\frac{\overline{U}_{\mathrm{N}}}{\overline{U}}=1 \tag{4}$$

In order to account simultaneously for elastic and elongational characteristics, the following non-dimensional parameter was introduced:

$$a=(3+n)^2\epsilon We^2\left(\frac{\overline{U}_{\mathrm{N}}}{\overline{U}}\right)^2 \tag{5}$$

Following previous work [15,16] we shall assume that the Fourier law for heat conduction is valid for the PTT viscoelastic fluid and that both the thermal conductivity k and the specific heat c_p are not affected by elasticity. With these assumptions, and once the hydrodynamic solution is known, our problem consists on the solution of the energy conservation equation:

$$\rho c_p u\frac{\partial T}{\partial x}=\frac{1}{r^n}\frac{\partial}{\partial r}\left(r^n k\frac{\partial T}{\partial r}\right)+\tau_{xr}\frac{\mathrm{d}u}{\mathrm{d}r} \tag{6}$$

subjected to the following boundary conditions:

$$\begin{aligned} &T=T_0 \quad \text{for } x\leqslant 0 \quad \forall r\\ &\frac{\partial T}{\partial r}=0 \quad \text{at } r=0 \quad \forall x\geqslant 0 \end{aligned} \tag{7}$$

and either for given wall temperature:

$$T=T_{\mathrm{w}} \quad \text{at } r=R \quad \forall x>0 \tag{8}$$

or, for given wall heat flux (assumed positive when entering the duct):

$$+k\frac{\partial T}{\partial r}=q_{\mathrm{w}} \quad \text{at } r=R \quad \forall x>0 \tag{9}$$

In Eq. (6) the second term on the right-hand side corresponds to the important effect of viscous dissipation, which is relevant for the high viscosity fluids encountered in polymer processing.

2.1. Non-dimensional formulation

Non-dimensional quantities are denoted with an asterisk. Velocity is scaled with the average value $u^* = u/\overline{U}$, the radial (lateral) coordinate is scaled with the radius (half-height) $r^* = r/R$ and the axial coordinate is scaled as $x^* = x\alpha/R^2\overline{U}$, where α is the thermal diffusivity ($\alpha \equiv k/\rho c_p$) following the practice for the classical Graetz problem with a Newtonian fluid. Scaling of temperature depends on the type of boundary condition. When the wall temperature T_w is given, a non-dimensional temperature is defined in the usual way:

$$\theta \equiv \frac{T - T_0}{T_w - T_0} \tag{10}$$

and the Brinkman number, which is a measure of viscous dissipation, is defined as

$$Br \equiv \frac{\eta \overline{U}^2}{k(T_w - T_0)} \tag{11}$$

On the other hand, for the case of an imposed heat flux it is better to define a non-dimensional temperature as

$$\theta = \frac{T - T_0}{q_w R 2(2-n)/k} \tag{12}$$

where the denominator represents a temperature scale (q_w is given) and consequently the Brinkman number is defined differently, as

$$Br \equiv \frac{\eta \overline{U}^2}{q_w R 2(2-n)} \tag{13}$$

The velocity profile u^* is obtained directly from Eq. (2) and upon a first derivation we arrive at the non-dimensional velocity gradient profile:

$$\frac{du^*}{dr^*} = -\frac{3+n}{2}\chi 2r^*(1 + 2ar^{*2}) \tag{14}$$

These profiles, together with the shear stress variation given by Eq. (3), are introduced into the energy equation (6), giving the non-dimensional form of the energy equation:

$$\frac{\partial}{\partial r^*}\left(r^{*n}\frac{\partial\theta}{\partial r^*}\right) + r^{*n}(3+n)^2 Br\chi^2 r^{*2}(1+2ar^{*2}) = r^{*n}\frac{3+n}{2}\chi(1-r^{*2})\left[1 + a(1+r^{*2})\right]\frac{\partial\theta}{\partial x^*} \tag{15}$$

to be solved for $\theta(r^*, x^*)$. The boundary conditions can be cast under the fully compact form.

Condition at inlet:

$$\theta(r^*, 0) = 0 \tag{16}$$

Condition at the symmetry axis:

$$r^* = 0, \quad \frac{\partial\theta(r^*, x^*)}{\partial r^*} = 0 \tag{17}$$

Condition at the wall:

$$r^* = 1, \quad (1-m)\theta(1, x^*) + m\frac{\partial\theta(r^*, x^*)}{\partial r^*} = (1-m) + \frac{m}{2(2-n)} \tag{18}$$

for $m = 0$, given constant T_w; for $m = 1$, given constant q_w.

3. Method of solution

The set of Eqs. (15)–(18) is similar to that found in the classical Graetz problem (see a textbook, e.g. Eckert and Drake [1]), albeit more complicated due to the simultaneous treatment of the plane and axisymmetric cases and also of the given temperature or flux boundary conditions, the inclusion of viscous dissipation, and the fact that the velocity profile for the viscoelastic fluid is not as simple as the parabolic variation of the Newtonian fluid. In essence, we follow that same method of solution, based on separation of variables for the radial and axial variation, which then leads to an eigenvalue problem. Specifically, we adopt the separation solution method explained by Mikhailov and Özisik [17] which is particularly appropriate for a non-homogeneous problem like the one at hand, and gives the solution of the temperature distribution $\theta(r^*, x^*)$ as composed of various terms related to different physical effects.

For the heat-flux boundary condition case, there are terms for: the axial variation of the average bulk temperature $\theta_b(x^*)$; the asymptotic (long x) radial distribution of temperature $\theta_{\phi 0}(r^*)$ without, or with $\theta_{g0}(r^*)$, viscous dissipation effects; and the main decaying term $\theta_t(r^*, x^*)$. This last term is given as an infinite series in terms of the eigenvalues and eigenfunctions of the corresponding Sturm–Liouville equation similarly to the classical Graetz problem, whereas the first three terms are particular solutions of the non-homogeneous equation.

For the constant temperature boundary condition case the solution is also the sum of a particular solution of the non-homogeneous energy equation, a term related to the asymptotic (long x) radial distribution of temperature, and the general solution of the homogeneous energy balance which becomes an infnite series of eigenvalues and eigenfunctions of the corresponding Sturm–Liouville problem.

We shall omit the full details of the derivation which are very cumbersome (the specialised text of Mikhailov and Özisik [17] is a good guide for that) and limit ourselves to giving the final expressions for the solution in terms of the temperature distribution $\theta(x^*, r^*)$ and the

Nusselt number variation $Nu(x^*)$. These expressions are in terms of eigenvalues μ^2 and some functions y_k, and the numerical methods used for these preliminary calculations are first explained. In the results section the present solution is compared to published solutions which are valid for some limiting conditions (e.g. Newtonian fluid without viscous dissipation) thus serving to verify the correctness of the present derivation.

3.1. Eigenvalue problem

The solution of Eq. (15) is the sum of a general solution of the corresponding homogeneous equation (setting $Br = 0$ in the second term of the left-hand side) and of a particular solution of Eq. (15) ($Br \neq 0$). To obtain the solution of the homogeneous equation the technique of separation of variables is applied, by which $\theta(x^*, r^*) = \Psi(r^*)\phi(x^*)$, leading to the differential equations:

$$\frac{\mathrm{d}\phi(x^*)}{\mathrm{d}x^*} + \mu^2\phi(x^*) = 0 \tag{19}$$

and

$$\frac{\mathrm{d}}{\mathrm{d}r^*}\left(r^{*n}\frac{\mathrm{d}\Psi(\mu,r^*)}{\mathrm{d}r^*}\right) + \left\{\mu^2 r^{*n}\frac{3+n}{2}\chi(1-r^2)\right.$$
$$\left.[1+a(1+r^{*2})]\right\}\Psi(\mu,r^*) = 0 \tag{20}$$

subject to boundary conditions:

$$r^* = 0, \quad \frac{\mathrm{d}\Psi(\mu,r^*)}{\mathrm{d}r^*} = 0 \tag{21}$$

and

$$r^* = 1, \quad (1-m)\Psi(\mu,1) + mr^{*n}\frac{\mathrm{d}\Psi(\mu,r^*)}{\mathrm{d}r^*} = 0 \tag{22}$$

where $m = 0$ corresponds to $T = T_\mathrm{w}$ constant, and $m = 1$ to $q_\mathrm{w} =$ constant. Eq. (19) is readily integrated and depends of the eigenvalues (μ^2) that are determined as a part of the solution of Eq. (20) which has the form of a Sturm–Liouville equation [18]. To the final solution for $\theta(r^*, x^*)$, the solution of Eq. (19) contributes the decaying exponential function of the longitudinal coordinate $\mathrm{e}^{-\mu^2 x^*}$. The eigenvalues μ^2 have been evaluated numerically by means of a freeware Fortran code SLEDGE (Pruess and Fulton, Netlib, cited by Pryce [19]) which can be found in the internet. This code, amongst other features, solves the general problem:

$$\frac{\mathrm{d}}{\mathrm{d}X}\left(X^n\frac{\mathrm{d}Y}{\mathrm{d}X}\right) + \mu^2 f(X)Y = 0 \tag{23}$$

and provides very accurate results for the eigenvalues. The calculated eigenvalues were accurate to at least 12 significant digits and, for each combination of independent variables, 160 eigenvalues were obtained for the finite series that is a part of the thermal solution. Note that in our case the function $f(X)$ depends on the elasticity of the PTT fluid through both the parameter a and the mean velocity ratio $\chi = \overline{U}_\mathrm{N}/\overline{U}$. Therefore, we need to reapply the SLEDGE code in order to obtain a full set of eigenvalues whenever the Weissenberg number of the flow or the elongational parameter of the PTT model are changed. Clearly, the amount of work and complexity of the task are greatly enhanced when one passes from the Newtonian to the viscoelastic case, in view of the increased number of free parameters.

Once the eigenvalues are known, our objective is the determination of the normalized temperature distribution and of the Nusselt number which, as we will see in the next two subsections, depend on various functions y_k and their derivatives [17]. They are defined as

$$y_1(\mu,r^*) \equiv r^{*n}\frac{\partial\Psi(\mu,r^*)}{\partial r^*} \tag{24}$$

$$y_2(\mu,r^*) \equiv \Psi(\mu,r^*) \tag{25}$$

$$y_3(\mu,r^*) \equiv \frac{\partial y_1(\mu,r^*)}{\partial\mu} \tag{26}$$

$$y_4(\mu,r^*) = \frac{\partial y_2(\mu,r^*)}{\partial\mu} \tag{27}$$

and the notation $y_k(\mu,r^*)$ makes it plain that these functions of r^* are also dependent, in a parametric way, of the eigenvalues μ. By comparing with the original Sturm–Liouville equations (20), the following four coupled ordinary differential equations (ODE's) are derived:

$$\frac{\mathrm{d}y_1(\mu,r^*)}{\mathrm{d}r^*} = -\mu^2 r^{*n}\frac{3+n}{2}\chi(1-r^{*2}) \times [1+a(1+r^{*2})]y_2(\mu,r^*) \tag{28}$$

$$\frac{\mathrm{d}y_2(\mu,r^*)}{\mathrm{d}r^*} = \frac{y_1(\mu,r^*)}{r^{*n}} \tag{29}$$

$$\frac{\mathrm{d}y_3(\mu,r^*)}{\mathrm{d}r^*} = -\mu r^{*n}\frac{3+n}{2}\chi(1-r^{*2})[1+a(1+r^{*2})] \times [\mu y_4(\mu,r^*) + 2y_2(\mu,r^*)] \tag{30}$$

$$\frac{\mathrm{d}y_4(\mu,r^*)}{\mathrm{d}r^*} = \frac{y_3(\mu,r^*)}{r^{*n}} \tag{31}$$

which need to be solved subjected to the initial conditions:

$$y_1(\mu,0) = 0 \tag{32}$$

$$y_2(\mu,0) = 1 \tag{33}$$

$$y_3(\mu,0) = 0 \tag{34}$$

$$y_4(\mu,0) = 0 \tag{35}$$

This was accomplished with a standard ODE solver based on a fourth-order Runge–Kutta method taken from Press et al. [20].

At this point we are in possession of the eigenvalues and eigenfunctions that are required for the solution of the thermal entrance problem and can proceed to the presentation of expressions for the temperature and Nusselt number distributions. The two cases corresponding to the given wall temperature and imposed wall heat flux are treated separately. Additional details can be found in Ref. [17].

3.2. Solution for given T_w

The temperature distribution for this case is given by

$$\theta(r^*,x^*) = 1 - \frac{2^{(2+n)}a(r^{*6}-1)+(5+4n)(r^{*4}-1)}{(20+7n)/3}Br\chi^2 + 2\sum_{i=1}^{\infty}\frac{e^{-\mu_i^2 x^*}y_2(\mu_i,r^*)}{\mu_i y_4(\mu_i,1)y_1(\mu_i,1)}\left\{y_1(\mu_i,1)-(3+n)^2Br \times \int_0^1 \chi^2 r^{*(2+n)}(2ar^{*2}+1)y_2(\mu_i,r^*)\,dr^*\right\} \quad (36)$$

where the first two terms are related to the asymptotic solution ($x \to \infty$) with viscous dissipation and the last term is an infinite series resulting from the Sturm–Liouville problem where μ_i^2 are the eigenvalues. Note that for $x \to \infty$, the last term gives a non-zero finite value. In engineering calculations one is generally more interested in knowing how the heat flux at the duct wall varies with the axial distance. This can be expressed in a non-dimensional way by means of a Nusselt number defined as

$$Nu = \frac{hD_H}{k} = \left(\frac{\partial\theta}{\partial r^*}\right)_{r^*=1}\frac{2(2-n)}{1-\theta_b} \quad (37)$$

where we used the relation $D_H/R = 2(2-n)$ for the hydraulic diameter. Now, upon calculation of the bulk temperature θ_b and derivation of the temperature profile $\partial\theta/\partial r^*$, we arrive at the following rather long expression:

$$Nu(x^*) = 2(2-n)\left\{\frac{-(3+n)Br\chi + 2S_1}{-\left[\frac{24(54a^2+110a+55)}{1925}(1-n)+\frac{280a^2+540a+225}{270}n\right]Br\chi^3 + 2(n+1)S_2}\right\} \quad (38)$$

where we define the sums:

$$S_1 \equiv \sum_{i=1}^{\infty}\frac{e^{-\mu_i^2 x^*}}{\mu_i y_4(\mu_i,1)}\{y_1(\mu_i,1)-(3+n)^2BrI_i\} \quad (39)$$

and

$$S_2 \equiv \sum_{i=1}^{\infty}\frac{e^{-\mu_i^2 x^*}}{\mu_i^3 y_4(\mu_i,1)}\{y_1(\mu_i,1)-(3+n)^2BrI_i\} \quad (40)$$

and the integral:

$$I_i \equiv \int_0^1 \chi^2 r^{*(2+n)}(2ar^{*2}+1)y_2(\mu_i,r^*)\,dr^* \quad (41)$$

The integration involving function y_2 in Eq. (41) was carried out numerically by means of Romberg's integration procedure performed in conjunction with the extended trapezoidal method.

The task of computing the Nusselt number for this case, therefore requires the systematic application of the following procedure:

- For a given *We* and ϵ, calculate $\chi = \overline{U}_N/\overline{U}$ (Eq. (4)) and a (Eq. (5))
- For that a, obtain the eigenvalues μ_i (from Eq. (20))
- For each eigenvalue μ_i, compute:
  $y_1(\mu_i,1)$, $y_2(\mu_i,r^*)$ and $y_4(\mu_i,1)$ from the system of Eqs. (28)–(31), and
  I_i, from Eq. (41).
- Finally, obtain *Nu* from Eq. (38) for each axial position x^*.

In engineering applications it is frequently more advantageous to use the average Nusselt number evaluated between the inlet and a given location x^*, denoted $\overline{Nu}$. An expression for $\overline{Nu}$ is derived from an energy balance and yields an implicit equation:

$$x^*\overline{Nu}(x^*) = (2-n)^2\ln\left[\frac{2Br(\overline{U}_N/\overline{U})(n-2)(n+3)-\overline{Nu}(x^*)}{(\overline{\theta}-1)\overline{Nu}(x^*)+2Br(\overline{U}_N/\overline{U})(n-2)(n+3)}\right] \quad (42)$$

Solution of this equation must be obtained numerically, a complex procedure when the Nusselt number changes sign because this singularity gives rise to the existence of multiple solutions.

3.3. Solution for given heat flux q_w

In this case the boundary conditions involve derivatives of the dependent variable θ and are non-homogeneous. Standard methods of solving non-homogeneous partial differential equations by transforming the equa-

tions and by eigenfunction expansions (see chapters 7–9 in the book by Farlow [21]; also [17]) give the final temperature distribution as a sum of various contributions:

$$\theta(r^*,x^*) = \theta_b(x^*) + \theta_{\phi 0}(r^*) + \theta_{g0}(r^*) + \theta_t(r^*,x^*) \tag{43}$$

where the average (bulk) value raises linearly with x^* as imposed by an overall energy balance:

$$\theta_b(x^*) = (n+1)x^*\left[\frac{1}{2(2-n)} + (3+n)Br\chi\right] \tag{44}$$

the asymptotic ($x \to \infty$) radial temperature distribution without and with viscous dissipation are given by

$$\theta_{\phi 0}(r^*) = \chi^2\left[n\frac{760a^2+1224a+495}{2160} + (1-n)\frac{3636a^2+6380a+2805}{23100}\right] - \chi\frac{n+1}{2(2-n)}\frac{2^{n+1}a[r^{*6} - 9(5/3)^{(1-n)}r^{*2} + 8(7/4)^{(1-n)}] + 9(5/9)^{(1-n)}[r^{*4} - 4(3/2)^{(1-n)}r^{*2} + 3(5/3)^{(1-n)}]}{72(5/9)^{(1-n)}} \tag{45}$$

and

$$\theta_{g0}(r^*) = (3+n)Br\chi[2(2-n)\theta_{\phi 0}(r^*)] - Br\chi^2\frac{2^{(n+2)}a(r^{*6}-1) + (5+4n)(r^{*4}-1)}{(20+7n)/3} - Br\chi^3\frac{280(162/35)^{(1-n)}a^2 + 504(110/21)^{(1-n)}a + 225(88/15)^{(1-n)}}{270(385/54)^n} \tag{46}$$

and the eigenfunction expansion (from the Sturm–Liouville problem) is

$$\theta_t(r^*,x^*) = 2\sum_{i=1}^{\infty}\frac{e^{-\mu_i^2 x^*}y_2(\mu_i,r^*)}{\mu_i y_3(\mu_i,1)y_2(\mu_i,1)}\left\{\frac{y_2(\mu_i,1)}{2(2-n)} + (3+n)^2 BrI_i\right\} \tag{47}$$

with I_i from Eq. (41). In contrast to the previous case, the eigenfunction expansion tends to zero for large values of x^*, thus the particular solution of the non-homogeneous equation (15) is made up of the sum of the fully developed terms θ_b, $\theta_{\phi 0}$ and θ_{g0}. Details of the derivation are omitted for the sake of brevity, but essentially follow the steps outlined by Mikhailov and Özisik, as mentioned beforehand.

Recall that for this case the non-dimensional temperature θ is defined differently (cf. Eq. (12)) and hence the expression for the Nusselt number will also differ from that of the given wall-temperature case. We have

$$Nu = \frac{hD_H}{k} = \frac{q_w D_H}{k(T_w - T_b)} \tag{48}$$

and keeping with the temperature scale adopted for the present case, we obtain

$$Nu(x^*) = \frac{1}{\theta_w(x^*) - \theta_b(x^*)} \tag{49}$$

where $\theta_w(x^*) = \theta(1,x^*)$.

Therefore the expression used to evaluate the axial variation of the Nusselt number will be

$$Nu(x^*) = \frac{1}{\theta_{\phi 0}(1) + \theta_{g0}(1) + \theta_t(1,x^*)} \tag{50}$$

with

$$\theta_{\phi 0}(1) = \chi^2\left[n\left(\frac{19}{54}a^2 + \frac{17}{30}a + \frac{11}{48}\right) + (1-n)\left(\frac{303}{1925}a^2 + \frac{29}{105}a + \frac{17}{140}\right)\right] \tag{51}$$

$$\theta_{g0}(1) = Br\chi^3\left[n\left(\frac{1}{\chi^2}\right) + (1-n)\left(\frac{468}{385}a^2 + \frac{68}{35}a + \frac{27}{35}\right)\right] \tag{52}$$

and

$$\theta_t(1,x^*) = 2\sum_{i=1}^{\infty}\frac{e^{-\mu_i^2 x^*}}{\mu_i y_3(\mu_i,1)}\left\{\frac{y_2(\mu_i,1)}{2(2-n)} + (3+n)^2 BrI_i\right\} \tag{53}$$

The task of computing *Nu* now follows the procedure:

- For a given *We* and ϵ, calculate $\chi = \overline{U}_N/\overline{U}$ (Eq. (4)) and a (Eq. (5))
- For that a, obtain the eigenvalues μ_i (from Eq. (20))
- For each eigenvalue μ_i, compute: $y_2(\mu_i,1)$, $y_2(\mu_i,r^*)$ and $y_3(\mu_i,1)$ from Eqs. (28)–(31), and I_i, from Eq. (41).
- Evaluate $\theta_{\phi 0}(1)$ (from Eq. (51)), $\theta_{g0}(1)$ (from Eq. (52)) and $\theta_t(1,x^*)$ (from Eq. (53))

- Finally, obtain Nu from Eq. (50) for each axial position x^*.

For this case, it is not possible to derive an expression for the average Nusselt number equivalent to that found for the constant wall temperature situation. The average Nusselt number must be calculated from the integral of the local Nusselt number and it is given by

$$\overline{Nu}(x^*) = \frac{1}{x^*}\int_0^{x^*} \frac{\mathrm{d}x^*}{\theta_w - \overline{\theta}} \tag{54}$$

The accurate numerical determination of this integral requires data for values of x^* well below our lower limit of x^*. Thus it is not possible here to perform the integral, but that is not considered to be problematic because in this case the heat flux is a given quantity.

4. Results and discussion

In order to keep the study focused we shall concentrate on the case for the round pipe and discuss separately the results for the two types of boundary conditions, imposed heat flux q_w and imposed wall temperature T_w. It is also convenient for each boundary condition type, to separate the analysis of the situations of pipe heating ($Br > 0$) and cooling ($Br < 0$).

4.1. Given wall heat flux q_w

4.1.1. Pipe heating ($q_w > 0; Br > 0$)

For the Newtonian fluid, the variation of the Nusselt number with the dimensionless axial distance x' is shown in Fig. 1, where the Brinkman number is used as parameter. Along this section and in all graphs we use a standard definition $x' = x/D_H RePr$ for the normalized axial distance, instead of x^*; it is easy to see that this new x' is related to that used in the previous sections by $x' = x^*/4(2-n)^2$. In the case without viscous dissipation it is possible to compare the present results, based on Eq. (49), with the solution reported by Shah and London [22], which is shown by the crosses in the figure. A perfect match between the two is observed, giving support to the correctness of the implementation of the various codes used in the present work to calculate the eigenvalues, the eigenfunctions, and their derivatives. When the Brinkman number is greater than zero, there are no available results in the literature to use for comparison, as far as we are aware. Ou and Cheng [6] do present graphs for the other boundary condition, of fixed wall temperature. Viscous dissipation tends to decrease the Nusselt number, as a result of the relatively faster increase of the wall temperature in comparison to the bulk temperature (cf. Eq. (48)). For the viscoelastic fluid this effect of Br is similar.

Another check on the present results is provided by the Nusselt number for the Newtonian fluid in the fully developed region ($x' > 0.05$). It is possible to show that Eq. (50) gives the analytical expression $Nu = 48/(11 + 48Br)$ (e.g. [15]) when $a \to 0$ and $x \to \infty$; this is shown directly in Fig. 1 by comparing the thermally developed theoretical values given in the caption with the present results at $x' \approx 1$. We note here that all the results for Newtonian and non-Newtonian fluids pertain to $x' \geqslant 10^{-5}$. Accurate results of Nusselt number for smaller values of x' (the Lévêque solution, see [22, p. 105]) would

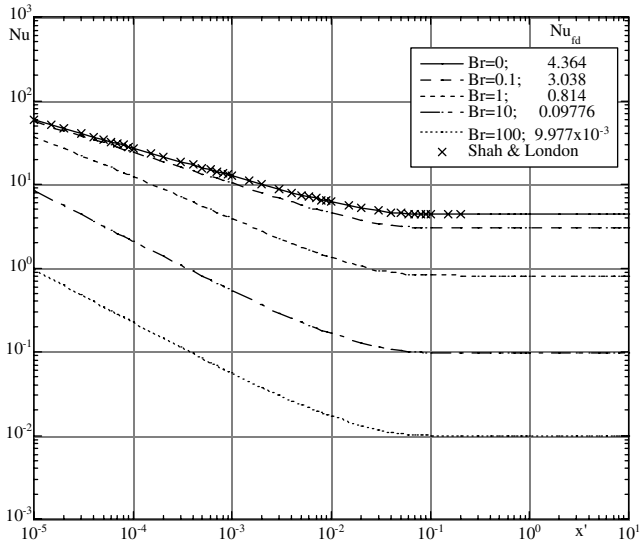

Fig. 1. Nusselt number vs. axial distance $x' = x/D_H RePr$, with Brinkman number as parameter. Newtonian fluid under imposed heat flux, positive q_w. The crosses are the solution given by Shah and London.

require a significant increase in the number of terms of the series, beyond the 160 that we used.

The influence of viscoelastic/elongational effects on the Nusselt number variation is shown in Fig. 2(a)–(c), for Brinkman numbers of 0, 1 and 10. It is emphasised that both elastic and elongational effects, acting in a coupled way, are important in changing the thermal characteristics from those for the Newtonian fluid. An elastic fluid with infinite molecular extensibility (corresponding to $\epsilon = 0$ in the PTT model) will show the same thermal response of the Newtonian fluid. In general, the parameter ϵWe^2 is seen to increase the Nusselt number, for any x' and Br, an expected feature due to the shear thinning in viscosity. This entails a flatter radial velocity profile with higher shear rates near, and better heat transfer at the wall, thus tending to reduce the temperature variation across the tube section with the consequence (Eq. (48)) that Nu will have the tendency to increase.

In an effort to compare our solution with existing data, Fig. 2(a) also shows results from Cho and Hartnett [23] which were based on theoretical expressions for power-law fluids that were validated experimentally, according to the review of [23]. In Fig. 2(a), the symbols representing the Nusselt number for power-law fluids with $n = 1/3$ (Eq. (28) of [23]) compare well with our values as ϵWe^2 increases because, as can be seen in [14], the viscometric viscosity of the PTT fluid behaves as that of a power-law fluid with an index $n = 1/3$ in the limit of high ϵWe^2 numbers. When the flow becomes thermally fully developed the Nusselt number is given by the expression (22) of Cho and Hartnett [23] which gives

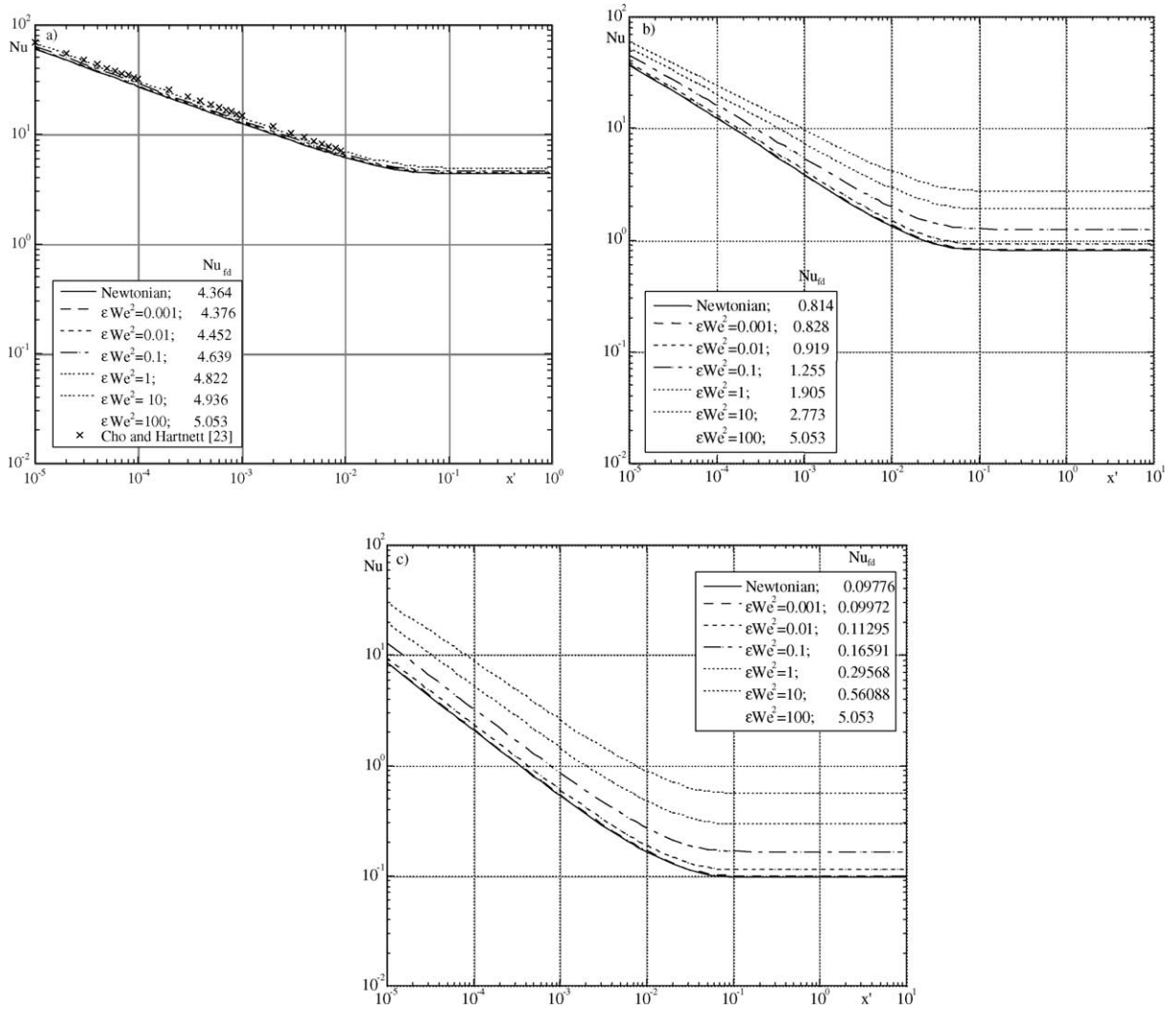

Fig. 2. Effect of viscoelasticity, measured by ϵWe^2, on the Nusselt number variation for various Brinkman numbers. Case of imposed wall heat flux, wall heating $q_w > 0$: (a) $Br = 0$, (b) $Br = 1$ and (c) $Br = 10$.

$Nu = 5.053$ for $n = 1/3$. According to these authors, provided the viscosity follows the specific power-law index, these Nusselt number results are equally valid for purely viscous and viscoelastic fluids.

An important feature is that the Nusselt number increase is greatly enhanced, in relative terms, when the viscous dissipation is taken into account (compare Fig. 2(a)–(c)). This is in agreement with previous findings for the thermally developed situation [15] and simply results from the fact that the rate of heat generated by viscous dissipation is proportional to the square of the shear rate which is high close to the tube walls. Further checks on the present solution are provided by a comparison between the asymptotic values on Fig. 2 (for $x' > 0.05$; see Table 1) and analytical results from Pinho and Oliveira (given in the captions of Fig. 2); again, the agreement is exact.

Table 1
Nusselt number data for imposed positive heat flux

x'	$Br = 0$	$Br = 0.1$	$Br = 1$	$Br = 10$	$Br = 100$
Panel A: $\epsilon We^2 = 0.1$					
1.00E−05	63.3	60.902	45.415	12.818	1.5675
2.00E−05	50.056	47.73	33.653	8.5211	1.0063
4.00E−05	39.562	37.32	24.716	5.6463	0.64784
6.00E−05	34.467	32.281	20.552	4.4354	0.50164
8.00E−05	31.253	29.11	18.001	3.7375	0.41882
1.00E−04	28.967	26.859	16.228	3.2731	0.36437
0.0002	22.88	20.888	11.712	2.1718	0.23747
0.0004	18.081	16.219	8.4168	1.4486	0.15611
0.0006	15.766	13.984	6.9329	1.1474	0.12278
0.0008	14.313	12.59	6.0433	0.97475	0.10384
0.001	13.284	11.608	5.435	0.86029	0.091353
0.002	10.572	9.0425	3.9278	0.5901	0.062131
0.004	8.485	7.1007	2.8767	0.41399	0.043301
0.006	7.5083	6.2055	2.4224	0.34135	0.035592
0.008	6.9126	5.6647	2.1582	0.30017	0.031238
0.01	6.5025	5.2952	1.9825	0.27322	0.028396
0.02	5.501	4.4041	1.5759	0.21233	0.021997
0.04	4.8988	3.8778	1.3485	0.17926	0.018537
0.06	4.726	3.7286	1.2861	0.17032	0.017603
0.08	4.6688	3.6795	1.2657	0.16742	0.0173
0.1	4.6492	3.6627	1.2588	0.16643	0.017197
0.2	4.6389	3.6538	1.2551	0.16591	0.017143
Panel B: $\epsilon We^2 = 10$					
1.00E−05	66.742	65.958	59.653	30.499	5.1804
2.00E−05	52.769	52.004	46.007	21.367	3.362
4.00E−05	41.697	40.956	35.31	14.844	2.1842
6.00E−05	36.323	35.598	30.175	11.958	1.6993
8.00E−05	32.933	32.22	26.963	10.246	1.4231
1.00E−04	30.522	29.818	24.695	9.0847	1.2409
0.0002	24.102	23.432	18.741	6.2426	0.81401
0.0004	19.043	18.41	14.172	4.2917	0.53836
0.0006	16.603	15.994	12.024	3.4534	0.42487
0.0008	15.072	14.48	10.701	2.9644	0.3602
0.001	13.988	13.41	9.7777	2.6363	0.31749
0.002	11.133	10.6	7.4099	1.848	0.21726
0.004	8.9377	8.4507	5.6701	1.3216	0.15245
0.006	7.912	7.451	4.888	1.1009	0.12586
0.008	7.2871	6.8439	4.423	0.97482	0.11083
0.01	6.8576	6.4276	4.109	0.89187	0.10101
0.02	5.8126	5.4189	3.3668	0.70332	0.078927
0.04	5.1924	4.8238	2.9433	0.60089	0.067075
0.06	5.0193	4.6583	2.8279	0.57369	0.063947
0.08	4.9639	4.6055	2.7913	0.56512	0.062964
0.1	4.9456	4.588	2.7792	0.5623	0.06264
0.2	4.9364	4.5792	2.7731	0.56089	0.062478

Table 2
Thermal entry data, x'_{95}, for imposed positive heat flux

Br	$\epsilon We^2 = 0$	$\epsilon We^2 = 1E{-}3$	$\epsilon We^2 = 1E{-}2$	$\epsilon We^2 = 1E{-}1$	$\epsilon We^2 = 1$	$\epsilon We^2 = 10$
0	0.043077	0.043038	0.042788	0.042062	0.041223	0.040645
0.1	0.045575	0.045495	0.04501	0.043679	0.042196	0.041165
1	0.049143	0.04906	0.04855	0.047109	0.045282	0.043585
10	0.050162	0.050089	0.04965	0.048477	0.047183	0.046158
100	0.050283	0.050212	0.049783	0.048656	0.047476	0.046689

For completeness and to make the present results more practical for a potential user, we present our data in Table 1 (Panel A) and (Panel B), for some of the most representative conditions. For other conditions the user may wish to visit the website indicated at the end of the paper, where additional tables and the codes used to generate the data are available.

Additionally, the distance x'_{95} required for establishment of fully developed thermal flow was determined, from the Nusselt number variation, and is listed in Table 2 for some conditions. The usual definition is used [22], i.e., x'_{95} corresponds to the position where $Nu(x' = x'_{95}) = 0.95Nu_{fd}$. It can be seen from Table 2 that viscous dissipation increases x'_{95} which, for a Newtonian fluid, varies from 0.043 at $Br = 0$ to 0.050 at $Br = 100$. Viscoelasticity has the opposite effect: say, for $Br = 1$, x'_{95} varies from 0.0490 for $\epsilon We^2 = 0$ to 0.0436 for $\epsilon We^2 = 10$.

4.1.2. Pipe cooling $(q_w, 0; Br < 0)$

The heat transfer trends for this situation, as far as influence of elasticity is concerned, essentially follow the lines of the heating case: Nu increases (in absolute terms) as ϵWe^2 increases. The variations are, however, more complicated due to the opposite influence of the imposed boundary conditions, tending to lower the fluid temperature, and viscous dissipation, tending to increase it. Below a certain critical value of the Brinkman number ($-Br_2$ of Pinho and Oliveira [15]; note change of sign in Br definition) the second influence starts becoming dominant, the Nu vs. x' curve reaches a singular point (when $\theta_b = \theta_w$, $Nu \to \infty$) and jumps from positive to negative values. This is illustrated in Fig. 3 for a value of $Br = -1$ and increasing values of the parameter ϵWe^2. The critical Brinkman number depends on ϵWe^2, tending to decrease as ϵWe^2 increases and, under certain conditions of high ϵWe^2, Nu remains positive for all x'. This is also shown in Fig. 3, where for the highest elastic/elongational fluid, $\epsilon We^2 = 10$, the Nusselt number remains positive, indicating that the fluid mean temperature stays all the time above the wall temperature (cf. Eq. (48), recalling that here $q_w < 0$).

The influence of the Brinkman number on the heat transfer characteristics has been discussed by Shah and London [22, pp. 129–132] for a Newtonian fluid, and by

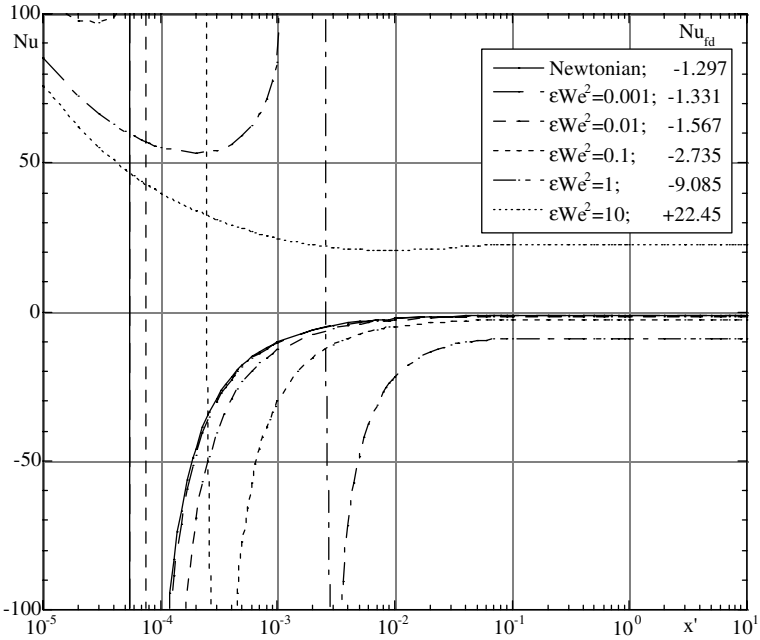

Fig. 3. Case of imposed negative wall heat flux (wall cooling, $q_w < 0$): effect of ϵWe^2 on the Nusselt number variation ($Br = -1$).

Pinho and Oliveira [15] for the PTT fluid under developed conditions. There are three possible situations, depending on the value of Br in relation to two critical values Br_1 and Br_2:

(1) $Br_1 < Br < 0$ ($Br_1 = -1/8$ for Newtonian fluid); wall cooling dominates over viscous dissipation, so both the bulk and the wall temperatures decrease with x', with $T_b > T_w$ (or, $\theta_b < \theta_w$), therefore giving a positive Nu. Contrary to the wall heating case, Nu increases with an increase of $|Br|$.
(2) $Br_2 < Br < Br_1$ ($Br_2 = -11/49$ for Newtonian fluid); viscous dissipation starts dominating the imposed wall cooling, so both T_b and T_w now raise with x'; however, the effect is not sufficient yet to raise T_w over T_b and so Nu remains positive for all x'. Same trends for Nu as in situation (1).
(3) $Br < Br_2$; viscous dissipation dominates completely, tending to raise T_w more sharply than T_b. So, there will be a critical position x'_{cr} where $\theta_w = \theta_b$ and $Nu \to \infty$; for $x' < x'_{cr}$, $T_w < T_b$ and the Nusselt number is positive; for $x' > x'_{cr}$, $T_w > T_b$ and Nu becomes negative.

The influence of elasticity/extensibility, as discussed in [15], is essentially to decrease (or increase, in absolute terms) the value of the transition Brinkman numbers: Br_1 and Br_2 will become more negative as ϵWe^2 is raised. The critical position x'_{cr} is also delayed to higher values and so Nu will tend to be positive all over the thermal entrance, as ϵWe^2 raises. In Fig. 3 that situation occurs for the curve at $\epsilon We^2 = 10$.

Again, for completeness we list in Table 3 some of the more representative results for the Nusselt number variation with x', with Br and ϵWe^2 as parameters, for this situation. Note the good agreement between the values in this table for large x' and the fully developed Nusselt numbers given in the caption of Fig. 3, which were based on theoretical results of [15]. In addition we give Table 4 which lists the development length x'_{95} for different values of ϵWe^2 and negative Brinkman numbers. It is seen that, depending on whether the Brinkman number is higher or lower than the critical value, the behaviour of the thermal entry length with the Brinkman number and viscoelasticity changes in a complex way.

4.2. Imposed wall temperature T_w

4.2.1. Fluid heating case ($Br > 0$)

This corresponds to the situation $T_w > T_0$ and so $Br > 0$. T_w is now fixed but the direction of heat transfer at the wall ($q_w = k(\partial T/\partial r)_w$) varies along the pipe when viscous dissipation is accounted for. For low x', heat transfer is from the wall to the fluid and, since T_w is then larger than T_b the Nusselt number is positive ($Nu = D_H q_w/k(T_w - T_b)$). Viscous dissipation tends to increase the fluid temperature at any given cross-section but its effect is more strongly felt near the wall where the velocity gradients are steeper. So, at a certain axial position (x'_1) the radial temperature gradient at the wall vanishes ($(\partial T/\partial r)_w = 0 \Rightarrow q_w = 0$), but T_w is still greater than T_b; therefore, Nu becomes zero at $x' = x'_1$ and then negative for higher $x' > x'_1$ (because $q_w < 0$). Viscous dissipation keeps increasing the bulk temperature, so that it eventually (at $x' = x'_2$) becomes equal to the wall temperature ($T_b = T_w$) resulting in a singular Nu, which jumps from $-\infty$ to $+\infty$. This behaviour of the Nu vs. x' variation, for a Newtonian fluid, was discussed by Shah and London [22, pp. 110–111] and is represented in Fig. 4 for $Br = 0$ and $Br = 1$.

The effect of shear thinning (due to the elastic and elongational properties of the fluid) is to increase Nu and delay the transitions mentioned above (x'_1 and x'_2), as shown by the corresponding curves in the same Fig. 4, for $\epsilon We^2 = 1$ ($Br = 0$ and 1).

As in the case of constant wall heat flux (Section 4.1.1), in the entry flow region and for fully developed thermal flow, our results tend to those provided by Cho and Hartnett [23] for a power-law fluid with index of $n = 1/3$.

When viscous dissipation is considered, the asymptotic Nu (large x') is independent of Br; for a Newtonian fluid, it was found to be equal to $Nu_{fd} = 48/5 \approx 9.6$ by Ou and Cheng [6], and the present solution confirms that value. For the PTT fluid, Coelho et al. [16] found Nu_{fd} to be a function of ϵWe^2 only, independently of Br, giving an asymptotic $Nu \approx 12.14$ at $\epsilon We^2 = 1$, in agreement with the present analysis (see Fig. 4).

4.2.2. Fluid cooling case ($Br < 0$)

This case is characterised by a wall temperature smaller than the inlet temperature ($T_w < T_0$) and so the Brinkman number is negative ($Br < 0$). The influence of Br is similar for the Newtonian and the PTT fluids, as shown in Fig. 5 (for $\epsilon We^2 = 0$ and 10; $Br = 0$, -0.1, -1, -10 and -100), and results from a balance between the opposite effects of wall cooling and heating by viscous dissipation. Ou and Cheng [6] have discussed the Newtonian situation; they found two regimes separated by the critical Brinkman number $Br_1 = -6/5$. For $Br < Br_1$, viscous dissipation effects dominate completely the heat transfer and the Nusselt number decays monotonically with x' (except at very low x' and high absolute Br, due to the boundary condition at $x' = 0$). For $Br_1 < Br < 0$, the Nu vs. x' variation goes through a minimum at a certain critical axial position x'_c; for $x' < x'_c$, wall cooling is dominant and Nu decreases with x'. For $x' > x'_c$, on the other hand, viscous dissipation becomes predominant inducing a raising tendency on the Nu vs. x' variation. At high x', when the thermal condition

Table 3
Nusselt number data for imposed negative heat flux

x'	$Br = 0$	$Br = -0.1$	$Br = -1$	$Br = -10$	$Br = -100$
Panel A: $\epsilon We^2 = 0.1$					
1.00E−05	63.3	65.895	104.42	−21.544	−1.6492
2.00E−05	50.056	52.621	97.658	−12.92	−1.0484
4.00E−05	39.562	42.09	99.069	−7.9018	−0.66978
6.00E−05	34.467	36.97	106.74	−5.9726	−0.51668
8.00E−05	31.253	33.737	118.48	−4.9124	−0.43036
1.00E−04	28.967	31.435	134.73	−4.2288	−0.37377
0.0002	22.88	25.291	491.89	−2.6807	−0.2425
0.0004	18.081	20.426	−122	−1.7249	−0.15886
0.0006	15.766	18.068	−57.529	−1.3429	−0.12472
0.0008	14.313	16.582	−38.857	−1.1285	−0.10537
0.001	13.284	15.526	−29.911	−0.9883	−0.092627
0.002	10.572	12.725	−15.287	−0.66425	−0.06287
0.004	8.485	10.54	−8.9357	−0.45876	−0.043747
0.006	7.5083	9.5037	−6.8284	−0.3755	−0.035932
0.008	6.9126	8.8655	−5.7467	−0.32872	−0.031523
0.01	6.5025	8.4228	−5.0803	−0.29829	−0.028646
0.02	5.501	7.3258	−3.6899	−0.23009	−0.022174
0.04	4.8988	6.6494	−3.0003	−0.19342	−0.018678
0.06	4.726	6.4516	−2.8218	−0.18355	−0.017735
0.08	4.6688	6.3858	−2.7647	−0.18035	−0.017429
0.1	4.6492	6.3631	−2.7453	−0.17926	−0.017325
0.2	4.6389	6.3512	−2.7351	−0.17869	−0.01727
Panel B: $\epsilon We^2 = 10$					
1.00E−05	66.742	67.544	75.743	−354.33	−6.1323
2.00E−05	52.769	53.556	61.859	−112.37	−3.8529
4.00E−05	41.697	42.465	50.906	−51.542	−2.4399
6.00E−05	36.323	37.079	45.618	−35.007	−1.8746
8.00E−05	32.933	33.679	42.299	−27.123	−1.5577
1.00E−04	30.522	31.26	39.949	−22.447	−1.3507
0.0002	24.102	24.812	33.761	−12.952	−0.87298
0.0004	19.043	19.721	29.016	−7.8135	−0.57063
0.0006	16.603	17.26	26.812	−5.9132	−0.44779
0.0008	15.072	15.713	25.477	−4.8866	−0.37828
0.001	13.988	14.617	24.565	−4.2313	−0.33259
0.002	11.133	11.722	22.373	−2.7665	−0.22609
0.004	8.9377	9.4842	21.093	−1.8766	−0.15783
0.006	7.912	8.4337	20.747	−1.5255	−0.12999
0.008	7.2871	7.7916	20.675	−1.3309	−0.1143
0.01	6.8576	7.3491	20.711	−1.2054	−0.10408
0.02	5.8126	6.2679	21.249	−0.92786	−0.081131
0.04	5.1924	5.622	22.013	−0.78184	−0.068854
0.06	5.0193	5.441	22.3	−0.7437	−0.065619
0.08	4.9639	5.3829	22.399	−0.73173	−0.064602
0.1	4.9456	5.3637	22.432	−0.7278	−0.064268
0.2	4.9364	5.3541	22.449	−0.72583	−0.064101

Table 4
Thermal entry data, x'_{95}, for imposed negative heat flux

Br	$\epsilon We^2 = 0$	$\epsilon We^2 = 1E{-}3$	$\epsilon We^2 = 1E{-}2$	$\epsilon We^2 = 1E{-}1$	$\epsilon We^2 = 1$	$\epsilon We^2 = 10$
−100	0.05031	0.05024	0.04981	0.0487	0.04755	0.04682
−10	0.05044	0.05037	0.04995	0.04889	0.04788	0.0475
−1	0.052	0.05196	0.05175	0.05168	0.05542	0.02139
−0.1	0.0347	0.03502	0.03657	0.03885	0.03981	0.04002

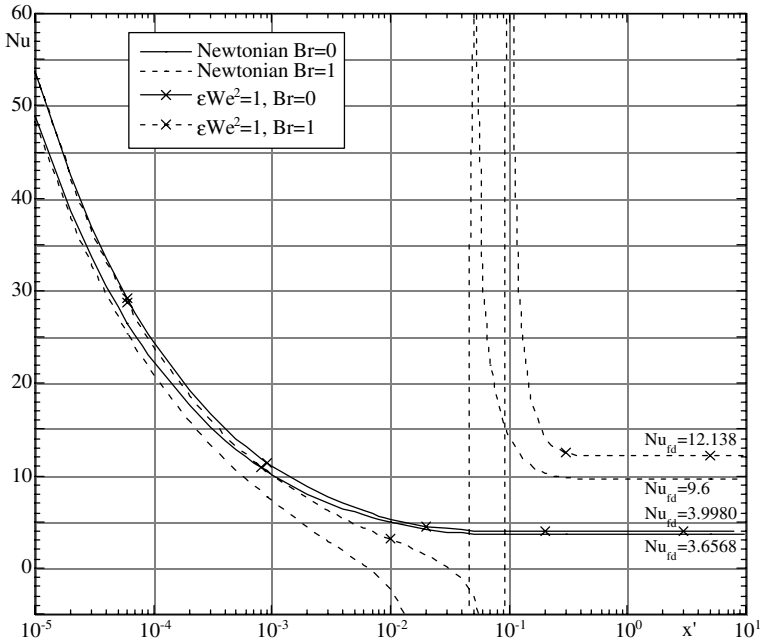

Fig. 4. Case of fixed wall temperature with fluid heating ($Br > 0$). Effect of viscous dissipation (Br) and elasticity/extensibility (ϵWe^2) on the Nusselt number variation with $x' = x/D_H RePr$.

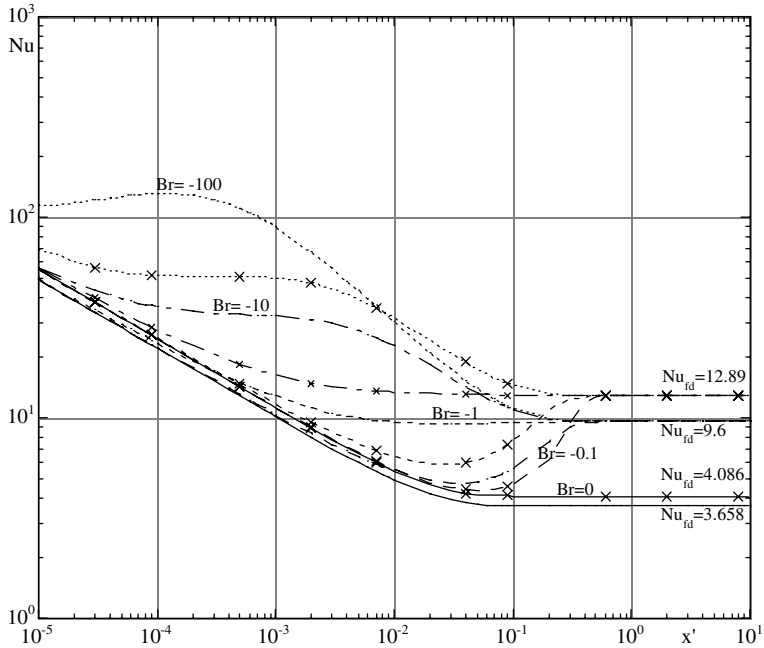

Fig. 5. Case of fixed wall temperature with fluid heating ($Br < 0$). Effect of viscous dissipation (Br) and elasticity/extensibility (ϵWe^2) on the Nusselt number variation with $x' = x/D_H RePr$. No symbols: Newtonian; crosses: $\epsilon We^2 = 10$.

becomes established (fully developed) Nu tends to a fixed level independent of Br; it was found to be $48/5 \approx 9.6$ for Newtonian fluids [22] and 12.9 for the viscoelastic PTT fluid as $\epsilon We^2 \to \infty$ [16]. These asymptotic values

Table 5
Thermal entry data, x'_{95}, for imposed wall temperature

Br	$\epsilon We^2 = 0$	$\epsilon We^2 = 1E{-}3$	$\epsilon We^2 = 1E{-}2$	$\epsilon We^2 = 1E{-}1$	$\epsilon We^2 = 1$	$\epsilon We^2 = 10$
−100	0.16397	0.16363	0.16158	0.15649	0.15103	0.14575
−10	0.15753	0.15703	0.15394	0.14408	0.12202	0.0087724
−1	0.0046927	0.004248	0.0027064	0.16356	0.22466	0.27736
−0.1	0.0011023	0.0010884	0.0010082	0.34804	0.38462	0.42293
0	0.033388	0.033359	0.033178	0.032685	0.032144	0.031778
0.1	0.31391	0.31383	0.31279	0.30332	0.39827	0.40968
1	0.24999	0.25266	0.29022	0.29443	0.20156	0.29972
10	0.17134	0.17115	0.17005	0.1744	0.17328	0.19143
100	0.16534	0.16502	0.16317	0.15891	0.15562	0.15527

are well captured by the present solution (cf. Fig. 5, where the analysis of [16] gives $Nu_{fd} \approx 12.9$).

Another feature observed from Fig. 5, regarding the effects brought about by viscoelastic/elongational fluid properties, is that whereas under fully developed conditions Nu is higher for higher ϵWe^2, under developing conditions Nu tends to be lower for the more elastic fluids. This can be explained by the enhanced heat transfer at the wall in the viscoelastic fluid case, on account of the steeper velocity gradients there, which tends to elongate the region over which the imposed wall cooling takes place, before viscous dissipation sets in.

Finally, Table 5 gives the development lengths x'_{95} for the constant wall case for both situations of $Br > 0$ and $Br < 0$.

5. Conclusions

The equivalent "Graetz problem" for a viscoelastic fluid obeying the PTT constitutive equation is solved for both thermal boundary conditions of specified wall temperature or imposed heat flux, under plane or axisymmetric geometries. The solution is given in terms of the developing dimensionless temperature profile, θ vs. x', and the dimensionless heat transfer coefficient, $Nu(x')$, as infinite series of eigenvalues and constants which have been numerically determined to high precision for this Sturm–Liouville like problem.

For various representative conditions, of wall heating and cooling and for given q_w or T_w, that solution was discussed and the influence of viscous dissipation (related to the Brinkman number) and shear thinning (related to the elasticity of the fluid measured by ϵWe^2) was established. In general, as the dimensionless group ϵWe^2 (elongational/elastic effects) increases the gross heat transfer characteristics to the fluid tend to increase. Some exceptions and singular conditions are also identified and discussed.

This study involved a considerable amount of work to determine the eigenvalues and constants appearing in the expressions for Nu vs. x', θ_b vs. x' and θ_w vs. x'. A fraction of the Nusselt number and thermal entry data obtained during this study was included as tables, for representative conditions. But, in order to avoid extending considerably the present paper, we have decided to make available additional information (like data for the average Nusselt $\overline{Nu}$), both as data files and FORTRAN codes, which can be accessed freely from the internet (at http://www.fe.up.pt/~fpinho/research/sturmptt.html).

References

[1] E.R.G. Eckert, R.M. Drake, Analysis of Heat and Mass Transfer, McGraw-Hill, New York, 1972.
[2] L. Graetz, Uber die Wärmeleitungsfähigkeit von flüssigkeiten. Part 1, Ann. Physik Chem. 18 (1883) 79–94.
[3] L. Graetz, Uber die Wärmeleitungsfähigkeit von flüssigkeiten. Part 2, Ann. Physik Chem. 25 (1885) 337–357.
[4] W. Nusselt, Die abhängigkeit der wärmeübergangszahl von der rohrlänge, Z. Ver. Deut. Ing. 54 (1910) 1154–1158.
[5] G.M. Brown, Heat or mass transfer in a fluid in laminar flow in a circular or flat conduit, A.I.Ch.E. J. 6 (2) (1960) 179–183.
[6] J.-W. Ou, K.C. Cheng, Viscous dissipation effects on thermal entrance heat transfer in laminar and turbulent pipe flows with uniform wall temperature, ASME paper 74-HT-50, 1974.
[7] R.B. Bird, R. Armstrong, O. Hassager, Dynamics of Polymeric Liquids, vol. 1, Fluid Mechanics, John Wiley, New York, 1987.
[8] E.B. Christiansen, G.E. Jensen, F.-S. Tao, Laminar flow heat transfer, A.I.Ch.E. J. 12 (6) (1966) 1196–1202.
[9] E.B. Christiansen, S.E. Craig Jr., Heat transfer to pseudoplastic fluids in laminar flows, A.I.Ch.E. J. 8 (2) (1962) 154–160.
[10] G. Forrest, W.L. Wilkinsson, Laminar heat transfer to power law fluids in tubes with constant wall temperature, Trans. Inst. Chem. Engrs. 51 (1973) 331–338.
[11] N. Phan-Thien, R.I. Tanner, A new constitutive equation derived from network theory, J. Non-Newt. Fluid Mech. 2 (1977) 353–365.
[12] L.M. Quinzani, R.C. Armstrong, R.A. Brown, Use of coupled birefringence and LDV studies of flow through a

planar contraction to test constitutive equations for concentrated polymer solutions, J. Rheol. 39 (1995) 1201–1228.
[13] G.W.M. Peters, J.F.M. Schoonen, F.P.T. Baaijens, H.E.H. Meijer, On the performance of enhanced constitutive models for polymer melts in a cross-slot flow, J. Non-Newt. Fluid Mech. 82 (1999) 387–427.
[14] P.J. Oliveira, F.T. Pinho, Analytical solution for fully-developed channel and pipe flow of Phan-Thien—Tanner fluids, J. Fluid Mech. 387 (1999) 271–280.
[15] F.T. Pinho, P.J. Oliveira, Analysis of forced convection in pipes and channels with the simplified Phan-Thien—Tanner fluid, Int. J. Heat Mass Transfer 43 (2000) 2273–2287.
[16] P.M. Coelho, F.T. Pinho, P.J. Oliveira, Fully developed forced convection of the Phan-Thien—Tanner fluid in ducts with a constant wall temperature, Int. J. Heat Mass Transfer 45 (7) (2002) 1413–1423.
[17] M.D. Mikhailov, M.N. Özisik, Unified Analysis and Solutions of Heat and Mass Diffusion, Dover, New York, 1994.
[18] E. Kreyszig, Advanced Engineering Mathematics, eighth ed., John Wiley, 1999.
[19] J.D. Pryce, Numerical Solution of Sturm–Liouville Problems, Claredon Press, Oxford, 1993.
[20] W.H. Press, S.A. Tenkolsky, W.T. Vetterling, B.P. Flannery, Numerical Recipes in Fortran, second ed., Cambridge University Press, 1992.
[21] S.J. Farlow, Partial Differential Equations for Scientists and Engineers, John Wiley and Sons, New York, 1982.
[22] R.K. Shah, A.L. London, Laminar Flow Forced Convection in Ducts, Academic Press, New York, 1978.
[23] Y.I. Cho, J.P. Hartnett, Non-Newtonian fluids, in: W.M. Rohsenow, J.P. Hartnett, E.N. Ganic (Eds.), Handbook of Heat Transfer Applications, McGraw-Hill, 1985 (Chapter 2).